Experimental determination of photoelectron angular distributions for $6S_{1/2} \rightarrow \epsilon P$ photoionization of Cs near the Cooper minimum

Yi-Yian Yin and D. S. Elliott
School of Electrical Engineering, Purdue University, West Lafayette, Indiana 47907
(Received 3 February 1992)

We have measured photoelectron angular distributions for the single-photon ionization of cesium at various wavelengths in the range from 313.5 to 266 nm. The photoelectron-angular-distribution asymmetry parameter β shows strong variations with energy, in contrast to nonrelativistic prediction of $\beta=2$. This variation is due to the spin-orbit interaction of the continuum electron. This effect is particularly dramatic near the Cooper minimum. From these results we determine the Fano parameter, providing confirmation of the semiempirical results of Norcross [Phys. Rev. A 7, 606 (1973)] for this range of energies.

PACS number(s): 32.80.Fb

The importance of spin-orbit coupling in the heavy alkali metals has long been recognized. Fermi [1] showed that this perturbation is responsible for the anomalous doublet-line-strength ratio for the $6\,^2S_{1/2} \rightarrow n\,^2P_j$ ($j=3/2$ and $1/2$) transition series in cesium in 1930. The line-strength ratio deviates from its nonrelativistic value of 2:1 due to the attractive (repulsive) spin-orbit interaction for the $^2P_{1/2}$ ($^2P_{3/2}$) states, leading to a contraction (expansion) of the corresponding radial wave functions. The electric dipole moments for the transitions from the ground state to the $n\,^2P_j$ series are thus significantly altered. This effect has also been used to explain and/or predict a number of interesting effects in photoionization. Seaton [2] explained the nonzero minimum of the photoionization cross section of heavy alkali metals in terms of a difference in electron energy for the Cooper minimum for the two fine-structure channels. Fano [3] predicted that a large photoelectron spin polarization would result from photoionization of unpolarized atoms by circularly polarized photons, an effect observed experimentally by Heinzmann, Kessler, and Lorenz [4]. Baum, Lubell, and Raith [5] reported a related polarization effect at about the same time. Spin-orbit coupling in the alkali-metal atoms can also be probed by measuring photoelectron angular distributions [6–10]. Recently we reported experimental measurements of photoelectron angular distributions for rubidium [11], for which a strong variation was evident as the wavelength of the exciting laser approached that of a Cooper minimum. These results were in excellent agreement with measurements [5] and calculations [12] of spin-polarization effects.

In this report we discuss similar measurements that we have completed in atomic cesium. The Cooper minimum in cesium occurs at a lower energy than in rubidium, allowing observations over a wider range of wavelengths, and thus we were able to observe a wider variation of angular distributions. Cesium has been the atom of choice for many of the studies of spin-orbit effects, both theoretical [1,8–10,12–19] and experimental [4,5,20,21]. One reason for this is, of course, that cesium is the most massive nonradioactive alkali metal, and thus is a good system for studying this perturbation. Cesium is also of interest, however, since the energy at which the cross section for the $j=1/2$ channel vanishes occurs very close to the ionization threshold. The cross section for ionization remains relatively large throughout the region about the Cooper minimum [22], making cesium a good source of spin-polarized electrons. (The polarization is 100% at about $\lambda=295$ nm [4].)

The angular distribution of photoelectrons induced by linearly polarized radiation via an electric dipole transition is described by [23]

$$\frac{d\sigma}{d\Omega}=\frac{\sigma_{\mathrm{TOT}}}{4\pi}[1+\beta P_2(\cos\theta)]\ , \tag{1}$$

where β is the asymmetry parameter that characterizes the photoelectron angular distribution, θ is the angle between the radiation polarization direction and the photoelectron momentum direction, and $P_2(\cos\theta)=(3\cos^2\theta-1)/2$ is the second-order Legendre polynomial. The energy dependence of β is a result of the variation of, and the interference among, the various possible continuum waves in photoionization. For the alkali-metal atoms in the ground state, only $s \rightarrow p$ transitions are possible in an electric dipole interaction because there is no $l \rightarrow l-1$ transition in that case. If only the nonrelativistic Hamiltonian is considered, the photoelectron angular distribution is proportional to $\cos^2\theta$ (i.e., $\beta=2$), and the distribution is independent of energy. The spin-orbit interaction changes this result, however, since the relative magnitude of the photoionization cross sections to the ϵP_j ($j=3/2,1/2$) channels varies with energy. The asymmetry parameter can be written in the form [6]

$$\beta=2\frac{R_{3/2}^2+2R_{1/2}R_{3/2}\cos(\delta_{3/2}-\delta_{1/2})}{2R_{3/2}^2+R_{1/2}^2}\ , \tag{2}$$

where R_j is the radial matrix element for the $n\,^2S_{1/2} \rightarrow \epsilon\,^2P_j$ transition, and δ_j is the phase shift of the

wave function. Spin-orbit effects in the p continuum on δ_j are relatively small [8,9]. Quantum-defect determinations [24] in the bound-state spectra of cesium show that $\Delta=\delta_{3/2}-\delta_{1/2}$ is relatively constant for high n states. We will use this bound-state data $\cos\Delta=0.995$ for analysis of our results. In the absence of spin-orbit coupling, $R_{3/2}=R_{1/2}$ and the asymmetry parameter β reduces to 2. $R_{3/2}$ and $R_{1/2}$ are significantly affected by the spin-orbit perturbation, however, and as the photon energy is varied near the Cooper minimum, $R_{3/2}$ and $R_{1/2}$ each pass through zero, but at somewhat different energies. Because of the slight radial contraction of the $j=1/2$ wave function, the $nS_{1/2}\rightarrow\epsilon P_{1/2}$ amplitude vanishes at a lower energy than does the amplitude for the $j=3/2$ channel. Thus β is expected to decrease rapidly from its nonrelativistic value of 2. From Eq. (2) we see that when $R_{1/2}\rightarrow 0,\beta\rightarrow 1$. Beyond this zero point, $R_{1/2}$ is of opposite sign and of increasing magnitude while $R_{3/2}$ is decreasing. When $R_{1/2}\cong -\frac{1}{2}R_{3/2}$, β is zero and the distribution is completely isotropic. For negative β, the maximum photoelectron current is emitted perpendicular to the polarization of the light. After reaching a minimum value near -1, β increases with increasing energy to a final value of 2.

The experimental system for measuring photoelectron angular distributions, shown in Fig. 1, is similar to that described previously [11]. The dye-laser system in this experiment consists of a tunable oscillator with three stages of amplification, all pumped by the frequency-doubled output of a neodymium-doped yttrium aluminum garnet (Nd:YAG) laser. Using different dye solutions (R590, R610, and DCM) we obtained TEM_{00} mode

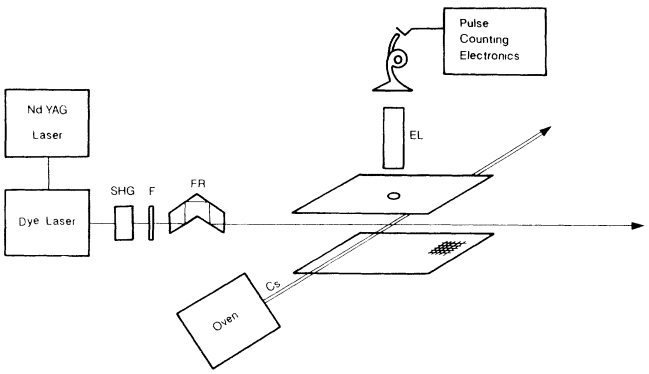

FIG. 1. Experimental setup. The tunable output of the Nd:YAG laser-pumped dye laser is frequency doubled in a second-harmonic-generating crystal (SHG). The visible radiation is absorbed and the uv transmitted by the filter (F), and the polarization of the uv beam is rotated by rotating the Fresnel rhomb (FR). The interaction region is defined by the intersection of the laser beam and the atomic cesium beam, the latter generated in a effusive oven. The interaction region is shielded by a pair of parallel conducting planes. The upper plane has an aperture behind which is mounted an electron lens (EL) and a channel electron multiplier. The pulse counting electronics determine the number of laser shots for which at least one electron is transmitted by the aperture.

output in the range from 550 to 627 nm. A β-BaB_2O_3 frequency-doubling crystal was used to generate a tunable ultraviolet (uv) laser beam in a range from 275 to 313.5 nm. The 266.0-nm data were obtained using the fourth harmonic of the Nd:YAG laser. We used a half-wave Fresnel rhomb (FR) to rotate the polarization of the uv beam. Through careful alignment of the rhomb and its axis of rotation, displacement of the laser beam in the interaction region was less than 0.2 mm. Polarization of the uv light exiting the rhomb was linear to within one part in a thousand.

The effusive atomic beam was generated in a two-stage oven. The cesium reservoir temperature was held at $\sim 160\,^{\circ}C$, governing the density of cesium atoms in the interaction area, which ranged from 1×10^7–5×10^7 atoms per cm^3. The temperature of the oven nozzle was slightly elevated (about 180 °C) to keep the cesium molecular content very small. After passing the interaction area, the cesium beam was evacuated by a turbomolecular pump, greatly reducing the background noise count rate.

The interaction area was shielded against perturbing electric fields by a pair of parallel conducting planes, both of stainless steel, one of sheet metal, the other of mesh (with 82% transmission and 50 threads per inch), which were electrically grounded. The planes were separated by $d=2.75$ cm. The upper plate had a 2.2-mm-diameter aperture, above which an electron lens and channel electron multiplier were mounted. The size of this aperture and that of the interaction region, defined by the intersection of the atom beam ($\phi\cong 2$ mm) and the laser beam ($\phi\cong 0.5$ mm) define the angular resolution of our measurements, which we estimate to be approximately 0.16 rad (9°). The earth's magnetic field in the interaction area was compensated to below 10 mG using three orthogonal pairs of Helmholtz coils of diameter 90 cm. The chamber was pumped by a 6-in. cryopump, which pulled the chamber pressure to 4×10^{-8} Torr. Use of a cryopump for this chamber reduced problems of stray fields that can result when using a diffusion pump, for example, due to thin coatings of pump oil inside the chamber. This is especially important for measurements of angular distributions of low-kinetic-energy electrons, where stray residual fields can influence measurements significantly.

The primary effect of any residual electric fields on our angular distribution measurements would be a change in the effective aperture size, thus influencing the angular resolution. Since a nonzero effective aperture size results in a relative increase of the isotropic part of the angular distribution, any stray fields that are present could cause a systematic error to our data. We determine an upper limit to the residual electric-field strengths in or surrounding our interaction volume using the results of related measurements we have made for two-photon ionizatio of cesium and rubidium. In these measurements we have photoionized the neutral atoms with photon energies as low as 20 meV over the ionization potential. Our ability to observe these photoelectrons establishes an upper bound on a repulsive stray field of $E\leq 20$ meV $\times(2/qd)$. An upper bound on an attractive stray field

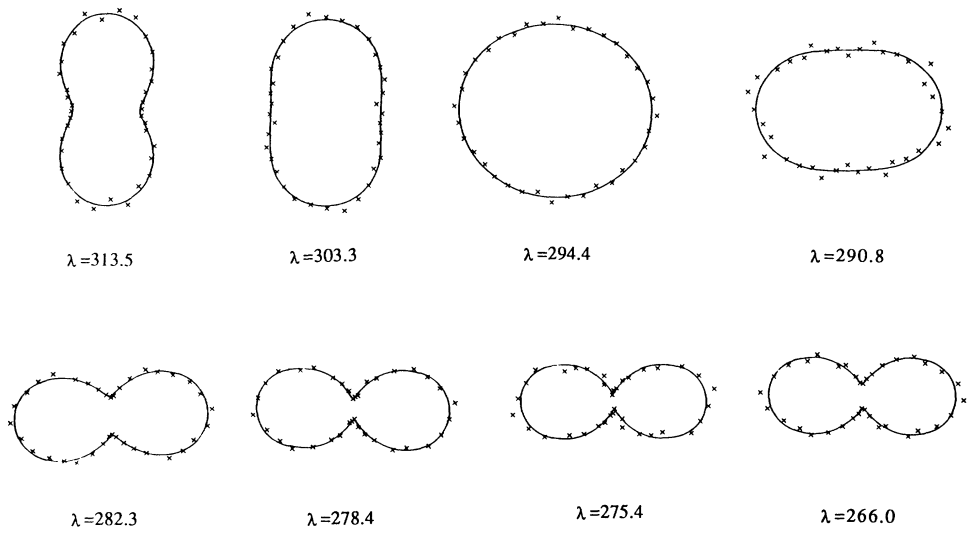

FIG. 2. Photoelectron angular distributions of cesium with light of wavelength from 266 to 313.5 nm. The laser polarization is in the vertical direction.

strength is also determined through these measurements, in that there is never a delayed electron pulse detected. An attractive potential would accelerate *toward* the detector those photoelectrons initially ejected *away* from the detector. These electrons would arrive significantly later than the electrons initially ejected toward the detector, resulting in a second time-delayed photoelectron pulse. The results of these measurements thus determine a maximum residual field strength in the interaction region, for which we calculate a negligible effect on our determination of β, even at the lowest photoelectron kinetic energies reported in this paper.

We have measured the cesium photoelectron angular distributions at eight different wavelengths near the Cooper minimum. The experimental photoelectron angular distributions are shown in Fig. 2. Measurements were made at wavelengths ranging from $\lambda=266.0$ to 313.5 nm. The photoionization threshold corresponds to a laser excitation wavelength of 318.4 nm for cesium. The crosses in Fig. 2 represent the average of the detection rates at angles θ and $\theta+180°$, and are determined from 2400 laser pulses per point. Each data point has been adjusted to correct for coincidence errors, assuming the electron detection is governed by Poisson statistics. These adjustments were minimized by restricting the maximum count rate to 0.3 counts per laser pulse. We estimate that less than 10 photoelectrons are produced per laser pulse, corresponding to ionization of $\sim 0.1\%$ of the atoms in the interaction volume. Space-charge effects are also minimized at these low excitation rates. The solid line for each distribution is the results of a least-squares fit of Eq. (1) to the data.

The measured asymmetry parameters β determined by Eq. (1) are given in Table I. These values have been adjusted for the effect of the finite aperture size and interaction volume. This is determined by averaging the square of the cosine of the angle θ over both these regions. For our experimental geometry the asymmetry parameter is effectively decreased by 0.7–0.9% by this angular resolution. $\Delta\beta_S$ reported here is purely statistical, and represents one standard deviation of the mean. The deviation of the data points from the fit is consistent with shot noise $\sigma \sim \sqrt{n}$, where n represents the number of detected electrons. The uncertainties reported in the column $\Delta\beta_T$ include a term that accounts for the background noise count rate determined by blocking the

TABLE I. Experimental results of these measurements, including asymmetry parameter β, the Fano parameter x, and uncertainties of each representing one standard deviation of the mean.

λ (nm)	ε (eV)	β	$\Delta\beta_s$	$\Delta\beta_T$	x	Δx
313.5	0.061	0.817	0.039	0.039	1.75	0.05
303.3	0.194	0.452	0.025	0.032	1.37	0.03
294.4	0.317	−0.068	0.014	0.031	0.95	0.02
290.8	0.370	−0.289	0.033	0.046	0.78	0.03
282.3	0.498	−0.727	0.020	0.068	0.44	0.06
278.4	0.559	−0.848	0.018	0.053	0.32	0.06
275.4	0.608	−0.889	0.050	0.086	0.27	+0.10,−0.15
266.0	0.767	−0.822	0.030	0.057	−0.35	0.06

atomic beam. These values were obtained by scaling $\Delta\beta_S$ by a factor $(1+r)$, where r represents the ratio of the standard deviation of the noise to the standard deviation of the signal data. We measured the background at a variety of angles θ, but no asymmetry was observable within the accuracy of these measurements. Thus the average background rate was subtracted from each data point in the distribution before the best-fit value of β was determined. The background rate increased in general as we decreased the wavelength, ranging from less than 0.002 counts per laser shot at $\lambda=313.5$ nm to about 0.02 counts per laser shot for $\lambda\sim280$ nm.

From Table I we note that the β values decrease as the Cooper minimum is approached and increase again after the minimum is passed. We plot the variation of β with energy in Fig. 3. The asymmetry parameter passes through zero near $\lambda=294.4$ nm, at which point the photoelectron angular distribution is nearly spherical. Beyond this point, as the laser wavelength continues to decrease, β becomes negative, corresponding to a maximum in the photoelectron angular distribution in the direction perpendicular to the laser polarization. β approaches $-1(R_{3/2}=-\frac{1}{2}R_{1/2})$, and then begins to increase again. With our present setup we are unable to generate wavelengths in the range below 266 nm, and so we cannot observe the angular distribution when $R_{3/2}\to0$ (at which point $\beta=0$). Our experiment does, however, clearly show the rapid variation of the angular distribution of the photoelectrons over a wide range of wavelengths near the Cooper minimum. We have also shown the theoretical results of Ong and Manson [8], and of Huang and Starace [9] in Fig. 3. The calculations of Huang and Starace were carried out in the length and velocity gauges, the former placing the Cooper minimum at too high an energy, while the latter places it too low. Huang and Starace used both frozen and relaxed ionic core wave functions. The results shown in Fig. 3 are those of the relaxed core calculations. The dot-dashed line in Fig. 3 is the asymmetry parameter for cesium as calculated by Norcross [15]. Agreement with these results is excellent.

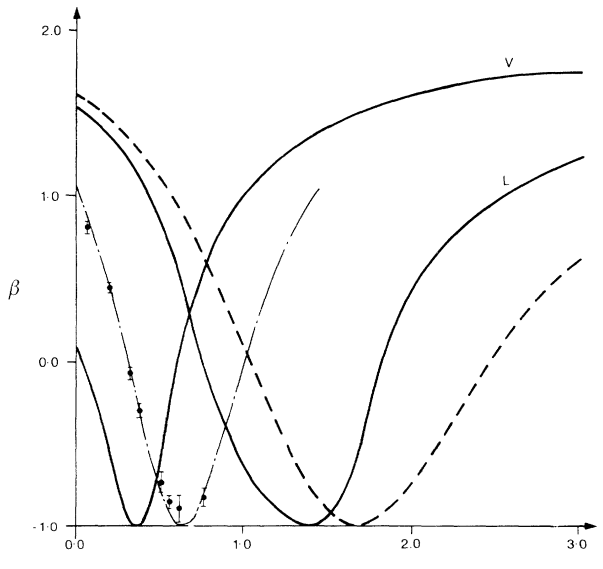

FIG. 3. Asymmetry parameter β for cesium $6^2S_{1/2}\to\epsilon P_j$ photoionization vs photoelectron energy ε. The data points represent the results of this work. Results of *ab initio* calculations of Ong and Manson [8], dashed line, and Huang and Starace [9], solid lines, are also shown. The latter were carried out in length (L) and velocity (V) gauges, the results of which are shown here. The dot-dashed line represents the results of calculations by Norcross [15] for the Fano parameter, which we have converted to β.

The data for the asymmetry parameter β as seen in Fig. 3 appears to have a minimum value greater than -1. The reason for this is not understood. Experimental artifacts such as the finite aperture size and residual electric-field effects have been carefully considered and accounted for in the data and their error bars. The quantum-defect phase shift Δ can result in $\beta_{\min}>-1$, but the magnitude of the phase shift necessary to fit the observations seems unreasonable. In the limit of small Δ, it can be shown that $\beta_{\min}\cong-1+4(1-\cos\Delta)/3$. Thus a minimum asymmetry parameter of -0.9, as indicated in Fig. 3, implies that $\Delta\cong0.12\pi$. This value is a factor of 4 larger than the value determined near threshold from bound-state data [24].

In Table I we have also shown our results for the Fano parameter $x(\varepsilon)$, which is a measure of the difference of the transition moments $R_{1/2}$ and $R_{3/2}$, $x(\varepsilon)=(2R_{3/2}+R_{1/2})/(R_{3/2}-R_{1/2})$. The asymmetry parameter β may be written in terms of x as $\beta=2[(x^2-1)-\frac{2}{3}(x+1)(x-2)(1-\cos\Delta)]/(x^2+2)$. Clearly when $\cos\Delta\cong1$ the sign of x cannot be determined from our measurements. As discussed earlier, we use $\cos\Delta=0.995$ to determine x from our data for β. The uncertainty Δx is derived from $\Delta\beta_T$. This uncertainty is asymmetric when x is small, as indicated for the $\lambda=275.4$ nm data point. The uncertainty is also relatively large in this region due to (i) the insensitivity of β to x near $x=0$, and (ii) the large $\Delta\beta_T$ resulting from the background noise rate for our measurements. We have plotted x as a function of the electron kinetic energy ε in Fig. 4. Our data is represented by the squares. We have also shown in Fig. 4 the results of the two other experimental determinations of x, as well as two semiempirical calculations. The x's indicate the data points from Heinzmann, Kessler, and Lorenz [4] as derived from their measurements of the Fano effect. When ionized with circularly polarized light, the spin polarization of the ejected electron P is given by [3] $P=[(2x+1)+\frac{4}{9}(x+1)(x-2)(1-\cos\Delta)]/(x^2+2)$. The uncertainties in x for these data are smallest in the region near $x=0$, as can be seen in Fig. 4, since the polarization depends most sensitively on x in these regions. The data points shown as open circles in Fig. 4 are derived from the measurements of the asymmetry in the photoionization current from a polarized cesium beam for left or right circularly polarized light, as determined by Baum, Lubell, and Raith [5]. The asymmetry in the current is given by $Q=2(x-1)/(x^2+2)$, leading to determination of x, so that these measurements are again expected to be

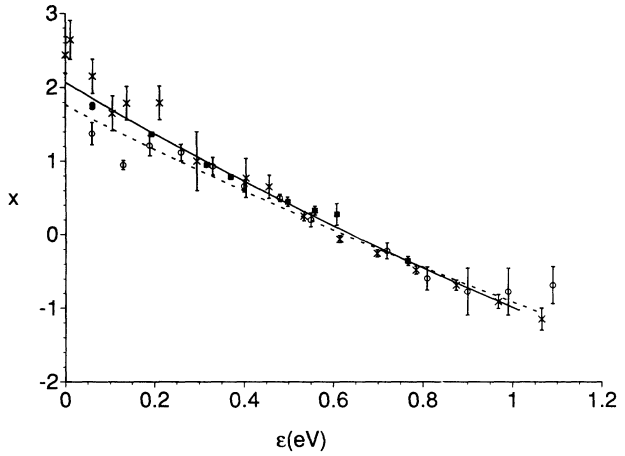

FIG. 4. The Fano parameter x as a function of photoelectron energy. The present data is shown by the square data points. The uncertainties of our data in the range $0.19<\varepsilon<0.4$ are less than the size of the squares. The results of Heinzmann, Kessler, and Lorenz are shown as x's, and those of Baum, Lubell, and Raith as circles. Also shown are the results of semiempirical calculations by Weisheit [12], dashed line, and Norcross [15], solid line.

most sensitive around $x=0$. These three data sets are generally consistent within quoted experimental uncertainties, except perhaps for $\varepsilon<0.2$ eV. The uncertainties for our data are comparable to those of the other two sets for $\varepsilon>0.4$ eV, and much smaller than the others for lower electron kinetic energies.

In principal, these three different photoionization measurements in cesium could be used in conjunction to determine $\Delta=\delta_{3/2}-\delta_{1/2}$ in the continuum. The parameters β and P each depend on x and Δ, while Q depends only on x, so any two of these data sets could yield the two parameters. In practice, however, this is difficult to do because of the uncertainty of the data sets and the small magnitude of $1-\cos\Delta$. For this reason, Δ is typically inferred from bound-state data, as we have done, and x is determined for each of these photoionization measurements individually.

The two solid lines in Fig. 4 are results of the semiempirical calculations of Weisheit [12] and Norcross [15]. Our data are in good agreement with the Norcross curve, which is also consistent with measurements in the bound-state spectra of the doublet-line-strength asymmetry [20]. The semiempirical works of Hofsaess [16] and Hansen [19] are also in excellent agreement in the bound-state region but do not report x in the continuum for comparison with our results. The results of *ab initio* calculations [13,14,17,18] for the Fano parameter in cesium are not in as good agreement. We have not shown these results in Fig. 4.

The final point we should like to address concerns the location of the energy at which $x=2$. The transition moment to the $P_{1/2}$ state vanishes at this point, and several papers have addressed this issue previously [4,5,15,20]. Specifically, the question was whether the x value at the threshold is greater than or less than 2. For $x>2$ at threshold, the zero of $R_{1/2}$ occurs in the continuum spectrum, while for $x<2$, this transition moment vanishes for a bound state. The data for the bound-state spectra reported in Ref. [20] strongly indicates that $x=2$ at an energy above the ionization threshold, a result in agreement with that of Norcross [15]. Subjecting our data for x vs ε to a linear-least-squares-fitting procedure, we determine that the best-fit value of x at threshold is 1.96 ± 0.06. Thus the present data seem to contradict the conclusion of Refs. [15] and [20] on this point, but they are not especially conclusive.

In conclusion, we have reported measurements of the energy dependence of the photoelectron angular distribution in cesium for single-photon ionization. The asymmetry parameter has the general shape expected on the basis of *ab initio* calculations but the energy of the minimum is not in agreement. The Fano parameter, derived from our angular distribution measurements, is in good agreement with the results of measurements of the Fano effect and with the calculated results of Norcross. The uncertainties of our measurements are significantly less than those of the previous measurements.

We are pleased to acknowledge support from NSF Grant No. PHY-9017244 for this work. Helpful discussions with C. Chen, A. V. Smith, and L. Westling are also gratefully acknowledged.

[1] E. Fermi, Z. Phys. **59**, 680 (1930).
[2] M. J. Seaton, Proc. R. Soc. London, Ser. A **208**, 418 (1951).
[3] U. Fano, Phys. Rev. A **178**, 169 (1969); **184**, 250 (1969).
[4] J. Kessler and J. Lorenz, Phys. Rev. Lett. **24**, 87 (1970); U. Heinzmann, J. Kessler, and J. Lorenz, Z. Phys. **240**, 42 (1970).
[5] M. S. Lubell and W. Raith, Phys. Rev. Lett. **23**, 211 (1969); G. Baum, M. S. Lubell, and W. Raith, *ibid.* **25**, 267 (1970); Phys. Rev. A **5**, 1073 (1972).
[6] T. E. H. Walker and J. T. Waber, Phys. Rev. Lett. **30**, 307 (1973); J. Phys. B **6**, 1165 (1973); **7**, 674 (1974).
[7] G. V. Marr, J. Phys. B **7**, L47 (1974).
[8] W. Ong and S. T. Manson, Phys. Rev. A **20**, 2364 (1979).
[9] K.-N. Huang and A. F. Starace, Phys. Rev. A **19**, 2335 (1979).
[10] M. S. Pindzola, Phys. Rev. A **32**, 1883 (1985).
[11] Yi-Yian Yin and D. S. Elliott, Phys. Rev. A **45**, 281 (1992).
[12] J. C. Weisheit, Phys. Rev. A **5**, 1621 (1972).
[13] I. L. Beigman, L. A. Vainshtein, and V. P. Shevelko, Opt. Spektrosk. **28**, 425 (1970) [Opt. Spectrosc. (USSR) **28**, 229 (1970)].
[14] J.-J. Chang and H. P. Kelly, Phys. Rev. A **5**, 1713 (1972).
[15] D. W. Norcross, Phys. Rev. A **7**, 606 (1973).

[16] D. Hofsaess, Z. Phys. A **281**, 1 (1977).
[17] B. N. Chichkov and V. P. Shevelko, Phys. Scr. **23**, 1055 (1981).
[18] M. Szulkin and J. Karwowski, J. Phys. B **14**, 4729 (1981).
[19] W. Hansen, J. Phys. B **17**, 4833 (1984).
[20] J. M. Raimond, M. Gross, C. Fabre, S. Haroche, and H. H. Stroke, J. Phys. B **11**, L765 (1978).
[21] L. E. Cuéllar, R. N. Compton, H. S. Carman, Jr., and C. S. Feigerle, Phys. Rev. Lett. **65**, 163 (1990).
[22] G. V. Marr and D. M. Creek, Proc. R. Soc. London, Ser. A **304**, 233 (1968).
[23] G. Wentzel, Z. Phys. **41**, 828 (1927).
[24] C.-J. Lorenzen and K. Niemax, J. Quant. Spectrosc. Radiat. Transfer **22**, 247 (1979).